Title: Phase Resetting Curves Determine Stability of Synchrony in One and Two Clusters of Pulse Coupled Oscillators with Delays

Authors: Ananth Vedururu Srinivas and Carmen C Canavier

Affiliation: Louisiana State University Health Sciences Center, Department of Cell Biology and Anatomy, New Orleans, LA, 70112

Corresponding Author: Ananth Vedururu Srinivas - avedur@lsuhsc.edu

Abstract

Previously, our group used phase response curves under a pulsatile coupling assumption to determine the stability of synchrony within a cluster of neural oscillators and between two clusters of oscillators. The interactions of the within and between cluster terms were considered, demonstrating how an alternating firing pattern between clusters could stabilize within cluster synchrony- even in clusters unable to synchronize themselves in isolation. In addition, criteria were derived for synchrony between two pulse coupled oscillators with synaptic delays. In this study, we update our previous work on one and two clusters of coupled oscillators to include delays and demonstrate the validity of the results using a map of the firing intervals based on the phase resetting curve. We use self-connected neurons to represent clusters and derive conditions under which an oscillator can phase-lock itself with a delayed input. Although this analysis only strictly applies to identical neurons receiving identical synapses from the same number of neurons, the principles are general and can be used to understand how to promote or

impede synchrony in physiological networks of neurons. Heterogeneity can be interpreted as a form of frozen noise, and approximate synchrony can be sustained despite heterogeneity. The pulse-coupled oscillator model can not only be used to describe biological neuronal networks but also cardiac pacemakers, lasers, fireflies, artificial neural networks, social self-organization, and wireless sensor networks.

Keywords: Pulse-Coupled Oscillators**;** Phase Response Curve; Synchronization; Phase-Locking; Phase resetting.

1. Introduction

Three mathematical methods that are commonly utilized for studying synchronization between neural oscillators [1,2] include weak coupling [3,4], firing time maps [5,6], and mean field methods, which often use leaky integrate-and-fire neurons [7]. The first two methods can only apply to repetitively firing neurons in which a baseline oscillation period can be measured, whereas the third method is most useful in the case in which individual neurons are not oscillators but instead emit spikes randomly. The first two methods employ different variants of phase response curves (PRCs). A phase response curve measures the change in length of the oscillation period caused by an input received during an oscillatory cycle. Weak coupling assumes that each oscillator remains very near its unperturbed trajectory, and the effects of multiple inputs are summed to get the averaged effect over one (unperturbed) oscillation cycle. In weak coupling, the infinitesimal phase response curve is obtained in the limit as the strength and duration of the synaptic input current both go to zero.

Here we focus on firing time maps under the assumption that coupling between neurons is pulsatile, meaning that the effect of the coupling is brief compared to the period of the neural network. The perturbation is not required to be small, but the oscillator is assumed to return to its unperturbed, free-running trajectory prior to receiving any additional inputs. In contrast to infinitesimal PRCs, phase response curves used for the firing maps are analogous to spike time response curves [8,9]; the perturbation used to measure the PRC is a post-synaptic conductance waveform, often assumed to be biexponential. Neural oscillators are nonlinear; therefore, the effect of a perturbation is not time invariant, but rather periodic with the same period as the neural oscillator. The PRC is the normalized change in cycle length plotted as a function of the phase of the oscillator. In a network in which each neuron receives N synaptic inputs, any given neuron can receive up to N simultaneous inputs. Since multiple inputs are not assumed to be additive, the PRC to *n* out of N inputs must be measured for each $n \in [0\,, N]$.

*1.1 Forced Oscillato*r: The simplest case of phase locking in pulse-coupled oscillators is that of a single oscillator forcing another oscillator in a one-to-one locking in which the driven oscillator receives an input on each cycle at a phase of φ. The criterion derived by [10] was stated in terms of the slope of the PRC at the locking phase φ. The slope $f'(\varphi)$ is simply the compensation in the direction back toward a steady phase locking normalized by the size of the perturbation away from the steady locking. For perfect compensation such that the locking is restored within a single cycle, the ratio of the compensation to the perturbation should be one; the stability criterion is $|1 - f'(\varphi)| < 1$. The perturbation away from the locking is multiplied by the factor $1 - f'(\varphi)$ on each cycle, therefore a slope of 1

results in a multiplier of 0. For stability, the perturbation must decay to zero, therefore for stability the absolute value of the factor must be less than one.

1.2 Synchrony Between Two Coupled Oscillators with and without delays: Previous work has derived the criterion for synchrony between two identical, reciprocally pulse-coupled oscillators in terms of the slope of the PRC at the phases of 0 and 1. Mapping the phases from 0 to around a circle, both 0 and 1 correspond to an upward threshold crossing that initiates an action potential, and is the phase at which an input is received by both neurons in a network with no delays. However, because of the definition of a cycle length as being between two action potentials threshold events, the PRC may have discontinuities. An input applied just before an action potential may delay that action potential, but an input applied after the action potential has already been initiated cannot. Therefore, the left and right slopes at the phase at which an input is received in the case with no delays can be different. The criterion for stability is [11] $|(1 - f'(0^+))\,(1 - f'(1^-))| < 1$. If inputs are received in different intervals, then they are multiplicative. However, if multiple inputs are received in the interval between a spike in one neuron and a spike in another neuron, then the compensations are additive; for a two neuron network the inputs are received by different neurons. Therefore with small delays (less than a network period), the criterion for stability of synchrony in reciprocally coupled identical neurons [12] becomes $|1 - f'(\delta/P_i) - f'(\delta/P_i)| < 1$, or equivalently $|1 - 2\,f'(\delta/P_i)| < 1$, where δ is the delay and P_i is the intrinsic period of the free running oscillator.

1.3 Alternating firing pattern in two neuron networks. The general criterion for stability of an alternating firing pattern between two neurons of neurons [13,14] A and B is $|(1 - f'_{A,B}(\varphi_A))\,(1 - f'_{B,A}(\varphi_B))| < 1$ where φ_A is the phase at which neuron A receives an input

from neuron B and φ_B is the phase at which neuron B receives an input from neuron A in a one-to-one phase-locked mode. The neurons are not presumed to be identical. The criterion is unchanged for short delays [12].

2. Methods

2.1 Model Neurons:

2.2.1 Fast-Spiking Inhibitory interneurons

For illustrative purposes we examined a model of a representative fast spiking parvalbumin (PV+) inhibitory interneuron in layers 2/3 of the medial entorhinal cortex [15]. This model was calibrated based on data the passive and active properties of these neurons, which have Hodgkin's class 2 excitability [16] meaning they cannot sustain repetitive firing below a threshold frequency. The single compartment model neurons have five state variables: the membrane potential, *V*, and four gating variables (m, h, n, and a) which use the same kinetic equations as the original Hodgkin-Huxley model [17,18], but with different parameters tuned to replicate the dynamics of fast spiking neurons in the medial entorhinal cortex and given in Table 1 of [15]. We also included two delayed rectifier K^+ currents (I_{Kv1} and I_{Kv3}), consistent with other models of fast-spiking interneurons [19,20]. All the synaptic parameters except one (synaptic decay constant) were calibrated according to [21] with a biexponential waveform in conductance with time constants of 0.3 and 0.45 ms and a peak conductance of 1.65 nS. The synaptic decay constant was 2.0 ms in [21] but was reduced to 0.45ms to reduce second order resetting. Two values for the synaptic reversal potential (-75 mV and -55 mV) were used to produce two very different phase resetting curves and the synaptic delay was varied to correspond to phases from 0.05 to 0.95 to test our stability criteria.

2.1.2 Excitatory Neurons

To understand the role of excitation on the network of fast-spiking inhibitory interneurons, we used the Reduced-Traub-Miles model (RTM model) [22,23] of an excitatory neuron in the rat hippocampus with a slight modification. Instead of applying a

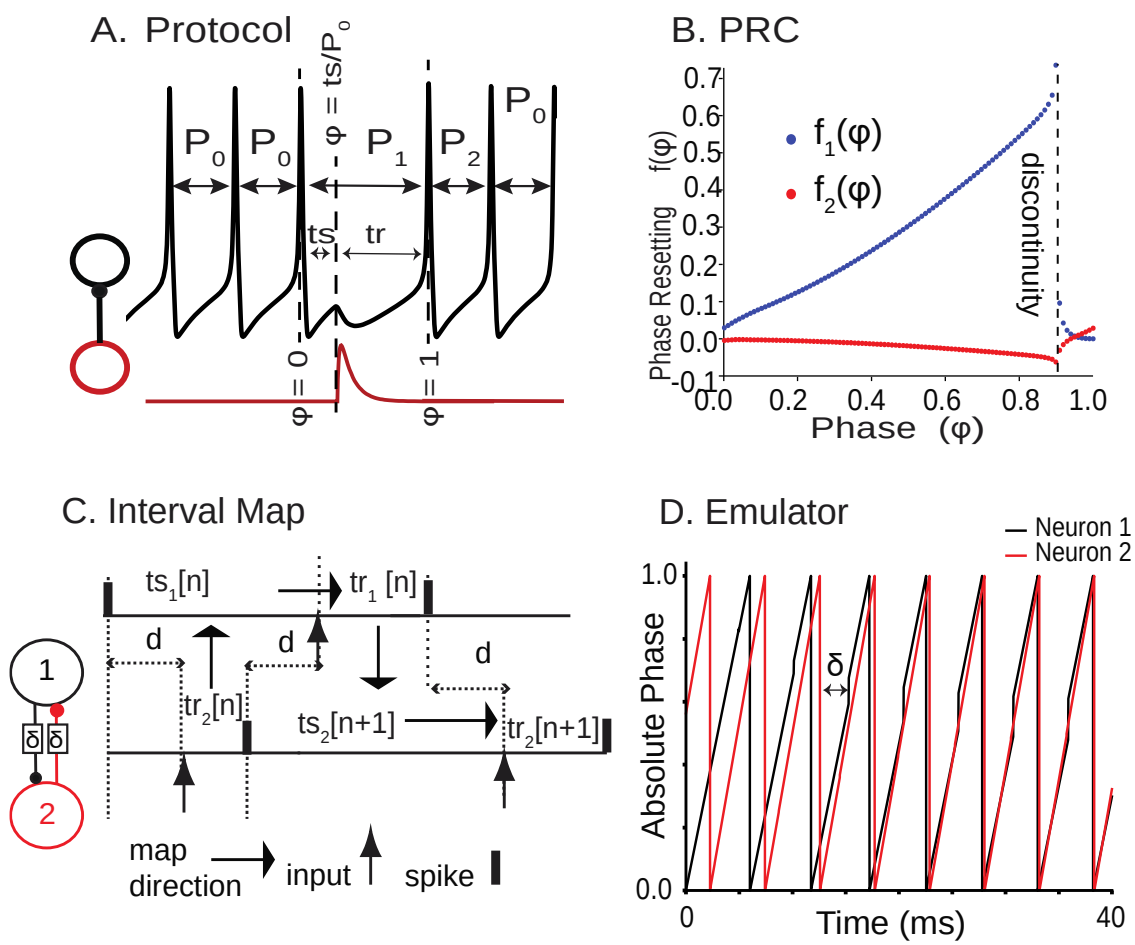

Fig. 1. Phase Response Curve Under Pulsatile Coupling Assumption. A. A single output waveform from one oscillator (red) is used to perturb the other at phases ranging from 0 (spike onset) to 1 (onset of the next spike). The phase φ is the stimulus interval (ts) normalized by the unperturbed period P_0. B. The phase resetting f(φ) is the normalized change in the cycle length caused by the perturbation $(P_1-P_0)/P_0$. The response interval tr is determined by the phase resetting $tr= P_0(1-\varphi+f(\varphi))$. C. The PRC defines an interval map in a two-neuron network with delays. The response interval in one neuron determines the stimulus interval in the other, which determines the next response interval in the same neuron. D. Depiction of the Emulator (map with no pre-determined firing order). Two neurons are shown to be driven towards synchrony. We can observe that the phase of each neuron increases linearly except when reaches its threshold value φ = 1 or when it has its phase reset after receiving a delayed input from the other neuron.

constant current to induce repetitive firing as in [23] we used a constant excitatory conductance to simulate channel rhodopsin drive as in [15].

2.2 *Phase response curves*: In Fig. 1AB we generated PRCs of the Via model for fast spiking neurons discussed in the Methods section, in response to hyperpolarizing inhibitory postsynaptic potentials. Except in the criterion for self-locking of an oscillator, we neglect resetting that occurs in cycles after the one in which the perturbation is received, for example second order resetting [14]. The first order phase response $f_{i,j}(\varphi)$ is defined as the normalized difference between the perturbed cycle period P_1 and the free-running intrinsic cycle period P_0 when a input from neuron j to neuron i is applied at a phase φ: $f_{i,j}(\varphi)=(P_1-P_0)/P_0$. The second order phase response $f_{2,i,j}(\varphi)$ is defined as the normalized difference between the period of the cycle P_2 following the perturbed cycle and the free-running period P_0 when a input from neuron j to neuron i is applied at a phase φ: $f_{2,i,j}(\varphi)=(P_2-P_0)/P$. Figure 1A defines the stimulus and response intervals based on the open loop PRC.

2.3 Stability Proofs: The basic idea is to assume a firing pattern (as the alternating firing pattern with delays in Fig. 1C) and create a discrete system of difference equations (a map or coupled set of maps) that characterize the dynamics in response to a perturbation. Then we linearize the map about the fixed point of the map and find the eigenvalues of the Jacobian matrix. These eigenvalues must have an absolute value less than 1 for stability. The maps rely upon the definition of stimulus and response intervals as defined in Fig.1. The stimulus interval $ts_i[n]$ in cycle *n* is the interval between when neuron *i* fires and when it next receives an input: $ts_i[n] = P_i\varphi_i[n]$, where P_i is the intrinsic period of neuron 1 and $\varphi_i[n]$ is the phase at which an input is received on cycle *n*. If two inputs are received

in the same cycle, the resetting due to the first input is assumed to be complete by the time the second input is received and the second stimulus interval is $ts_{i,2}[n] = P_i(\varphi_{i,2}[n] - \varphi_i[n] + f(\varphi_i[n]))$, where $\varphi_{i,2}$ is the phase at which the second input is received, and $f(\varphi_i)$ is the phase resetting due to the first input. The response interval $tr_i[n]$ is the interval between the receipt of the last input and the next spike in neuron *i*: $tr_i[n] = P_i(1 - \varphi_i[n] + f(\varphi_i[n]))$ if there has only been one input in the cycle and $tr_i[n] = P_i(1 - \varphi_{i,2}[n] + f(\varphi_{i,2}[n]))$ if there have been two.

2.4 Emulator (Map with no predetermined firing order [6]): The concept of a hybrid oscillator that updates its phase linearly between events but discontinuously when an input is received, or its threshold is crossed was pioneered by Winfree [24] and extended by others [25,26] . In this study, we present the modified Winfree Model for pulsatile coupling with delays:

$$\frac{d\varphi_i}{dt} = \omega - \sum_{j,k} D\left(t = t - t_{j,k} + \delta\right) f_{i,j}(\varphi_i) - D(\varphi_i = 1)$$

where ω is the angular frequency, φ_i is the phase of the ith neuron, $t_{j,k}$ is the time the kth input is received from neuron *j*, $f_{i,j}(\varphi_i)$ is the phase response of neuron i at time $t_{j,k}$ to in input from neuron *j* and the phase is reset to zero when the phase reaches 1. In this modified Winfree Model represented by the equation above, the function D() represents a unit impulse at the time the condition in parentheses is true and δ represents the synaptic delay. Since PRCs are not additive, at the time two neurons synchronize their input to neuron *i*, for strict accuracy the appropriate PRC corresponding to the joint input must be substituted for the two separate PRCs. We utilize the emulator to test our proofs

because the pulsatile coupling assumptions are honored exactly, whereas in simulations using conductance-based models we cannot ensure that the assumption of pulsatile coupling is strictly honored. Figure 1D shows two coupled PRCs converging to synchrony, using the emulator. The input given to this map is the intrinsic period and phase resetting curve of each neuron.

3. Results

3.1 Assumptions of Pulsatile Coupling. The phase response curve is measured under open loop conditions, meaning that there is no feedback to the rest of the circuit during the measurement. In order for the phase response curve measured under those conditions to apply to a closed loop circuit with feedback from other circuit elements, several assumptions must be honored: 1) The trajectory of each oscillator must be near enough to its unperturbed limit cycle when an input is received for the phase response curve to predict the timing of the next spike by subtracting the first order resetting from the current phase. 2) If there are multiple inputs within a network period, then the trajectory should be near the limit cycle at the time that each input is received. It is not required that the trajectory be near the limit cycle when a spike is emitted. 3) The second order resetting can be non-negligible only for the last input received within a network period. The second order resetting is assumed to be complete between the spike time and the receipt of the first input within a network period (the stimulus interval). 4) Third order resetting should be negligible. 5) There should be no non-negligible cumulative effect of multiple inputs such as firing rate adaptation or acceleration.

3.2 Self-connected oscillator with delay:

Previously, a self-connected oscillator has been taken as the equivalent to a network of identical, synchronized, mutually connected neurons [27]. One study derived existence and stability criteria for a periodically spiking neuron forcing itself with a feedback input at a fixed delay after each spike [28]. Their rationale was that excitatory pyramidal cells receive feedback from inhibitory interneurons, such that there were two conduction and synaptic delays in the feedback loop. They only considered delays longer than the network period and neglected second order resetting. However, the case of delays shorter than a network period has not previously been addressed. We formulated a simple existence criterion for a stable phase locking of an oscillator with intrinsic period P_i by feedback at a fixed delay (δ) after each spike is emitted.

Lemma: For the phase locked mode to exist, the stimulus interval at phase locking should be equal to the delay $\delta = P_i(\varphi^* + f_2(\varphi^*))$, where φ^* is the phase at which an input would arrive at phase locking.

Proof: If there is no second order resetting, the existence of a phase-locked mode is guaranteed at every delay less than the network period $\delta < P_i(1+ f_1(\varphi^*))$. This is because at the steady state, the phase defined by $\varphi^* = (ts[\infty]/P_i)$ at which the oscillator receives the input due to self-connection would be just the normalized delay δ/P_i.

However, if the delay δ is such that the input from the self-connection arrives late in the cycle, then the effect of second-order resetting becomes significant, especially in the case of the model neurons considered in this study.

Therefore, with the second order resetting, the phase at which the input from the self-connection is received is determined by the second order resetting. As a result, the

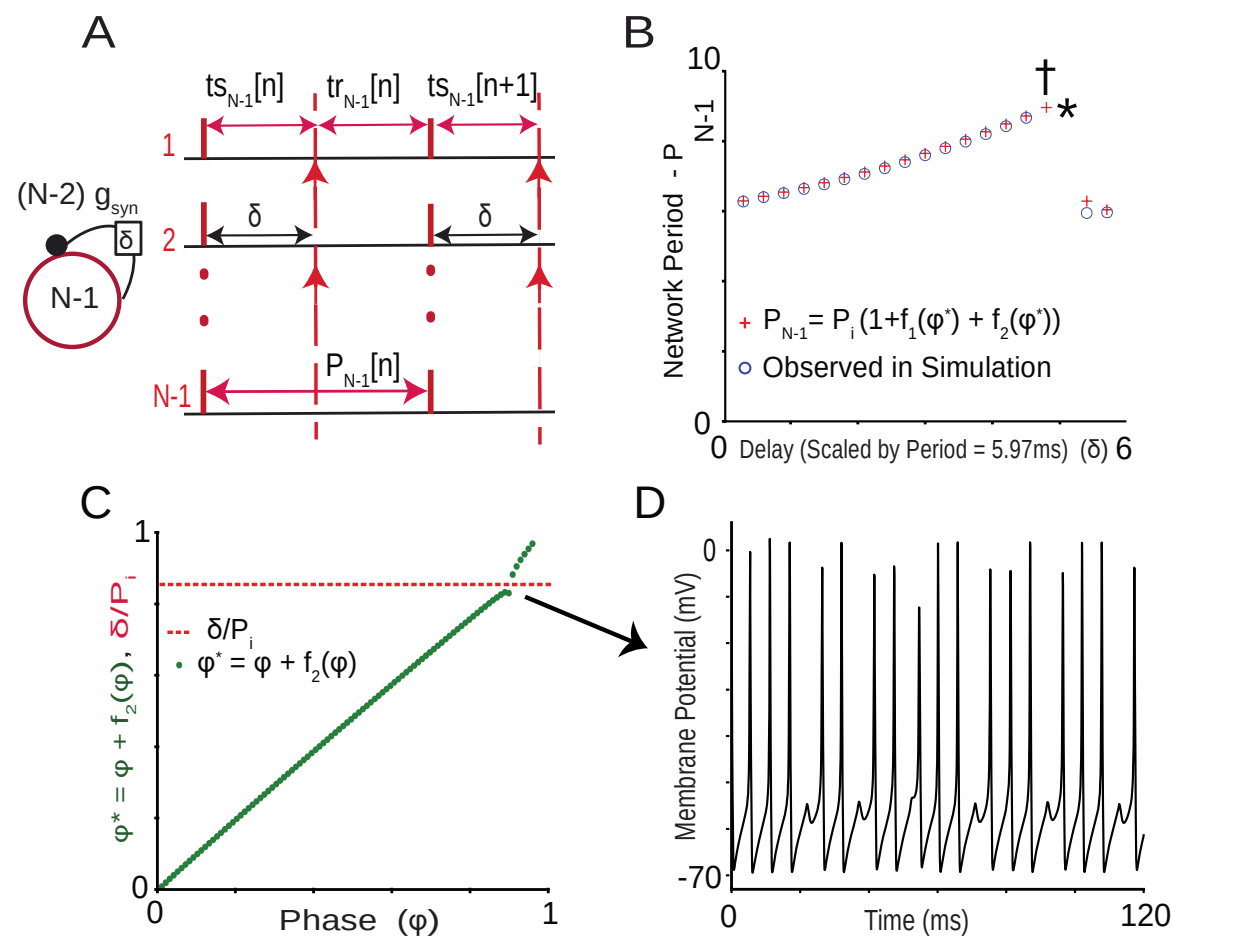

Fig. 2. A. Interval map for the self-connected oscillator. The sub-cluster of N-1 neurons from a cluster of N neurons receive N-2 inputs after a delay δ. B. Plot of predicted and observed periods for various delays at which the inputs from self-connection arrive. C. Plot of the steady-state stimulus interval ts[∞] = $\varphi^* + f_2(\varphi^*)$ versus the phase φ , to check the existence of phase-locking in self-connected oscillator. D. Trace of the membrane potential when δ = 5.1 ms. B (Inset): * denotes the case for the dashed red line in C for a delay of 5.1ms. In this case, the prediction is that there would no phase-locking in the self-connected oscillator. As a result, predicted period is not plotted for this delay. † denotes the case when the delay is 4.8 ms where the existence is predicted by the intersection (not shown here) and hence the predicted network period is plotted, but the numerical simulations of the model of the oscillator do not show periodicity in spiking. Thus, there is no observed period in the figure.

steady-state stimulus interval ts[∞] becomes a function of the second order resetting:

$$ts[\infty] = P_i(\varphi^* + f_2(\varphi^*))$$

where φ^* is the steady-state phase. But the input due to self-connection would arrive at a phase of δ/P_i. So, for phase locking to exist, these two quantities must be equal to each other:

$$\delta/P_i = P_i(\varphi^* + f_2(\varphi^*))$$

For the model neurons, we established existence using graphical method. We used a fast-spiking model neurons with intrinsic period P_i = 5.97 ms. As described in the Methods section, we varied the synaptic from 0.05* P_i (δ = 0.3 ms) to 0.95*P_i (δ = 5.7ms). Figure 2C depicts the case with δ = 5.1 ms such that $\delta/P_i \sim 0.90$. The green curve in the figure represents $P_i\,(\varphi^* + f_2(\varphi^*))$ whereas the red dashed line is the constant value $\delta/P_i \sim 0.9$. In this case, due to discontinuity in the second order resetting (figure 1B), we see that there is no intersection of the two curves, and hence, we conclude that the phase-locking does not exist for a delay of 5.1ms. For other delays we find that the curves intersect (not shown here) thereby establishing the existence of phase locking. If phase-locking exists, then the period of the self-connected oscillator can be predicted using the relation: $P^*_{N-1} = (1 + f_1(\varphi^*) + f_2(\varphi^*))$. In figure 2B, we plotted the periods predicted through this relation for each delay in the arrival of input stimulus due to self-connection versus the delay. We also plotted the periods observed from simulating these oscillators using systems of ODEs for various delays. Two cases are to be noted (see Figure 2B):

1. * in the inset of the figure denotes the case for which the delay is 5.1ms and existence is not predicted, thus we have not indicated any predicted period in that case.

2. For the case in which the input from the self-connection arrives at a delay of 4.8ms, we observe a special case in which the existence is established by the intersection of curves but from the ODE simulations we do not observe a one-to-one locking of the neuron by itself. Assumption 3 above is violated because the second order resetting is not completed in the stimulus interval but instead continues into the response interval, rendering the prediction invalid indicated by **†** in figure 2B.

In a network of identical identically connected neurons, synchrony always exists due to the symmetry [29]. Fig. 1D shows that synchrony need not be periodic.

The stability criterion for phase locking in self-connected oscillators is identical for self-forcing as for external forcing: $-1 < 1-f'_1(\varphi^*)-f'_2(\varphi^*) < 1$ [30].

3.3 Extension of the results for synchrony in an N neuron network without delay to include delays:

For a network of neurons each receiving N-1 identical pulse-coupled inputs, the criteria for synchrony in a network with no delays, under the assumption that the most destabilizing perturbation is to perturb a single neuron from a synchronous cluster, are $\left|(1-f'_{1,N}(0^+))(1-f'_{N-1,1}(1^-))\right|<1$ and $\left|(1-f'_{N-1,1}(0^+))(1-f'_{1,N-1}(1^-))\right|<1$ (Canavier and Achuthan, 2010). Here, the synchronous cluster is assumed to have N-2 self-connections representing the inputs from all the neurons in the presumed synchronous cluster. There are indices *i,j* on the phase resetting curve, where *i* is 1 for the PRC of the single neuron in response to a *j* equal to N-1 inputs from the presumed synchronous cluster and i is N-1 for the PRC of presumed synchronous cluster in response to a *j* equal to 1 inputs from N-1 the single neuron.

In this study, we extend this criterion by analogy with the two-neuron case with delays as studied in [12]. Figures 3A and 3B depict the perturbations with synaptic delays. In the representation of the synchronous cluster, we incorporate inputs due to self-connections but not autapses (synapses from an individual neuron onto itself). However, the results that we will prove can be easily extended to include autapses. Connections need not be all to all as long as each neuron receives the same number of identical inputs [15].

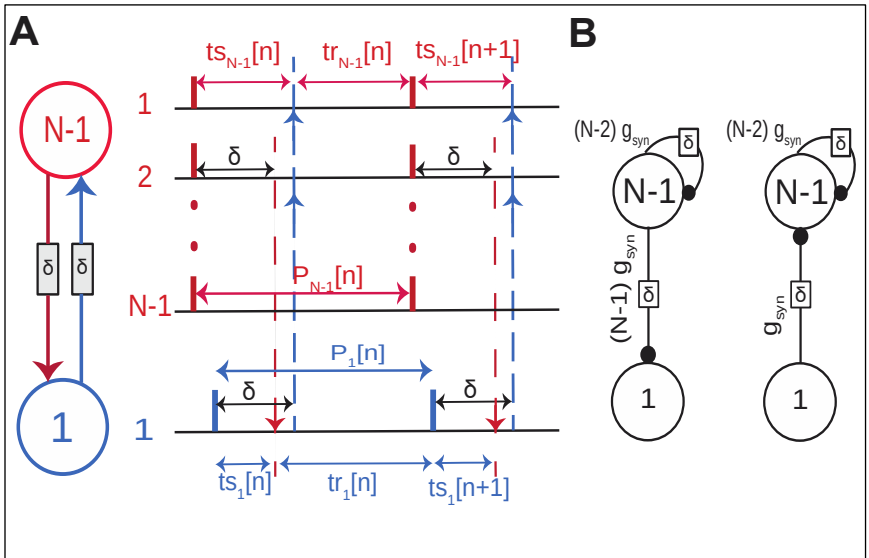

Fig. 3. Stability of Synchrony in a Network of N identical neurons each receiving N-1 identical inputs. A. Schematic firing pattern in which a single neuron is perturbed from synchrony. These intervals are used in the proof of stability. B. Reduction of the network to two oscillators. The larger group is assumed to receive delayed synchronous feedback from itself. Autapses are not considered.

Let P_i be the intrinsic period of the single perturbed neuron and let P_{N-1} denote the network period of the N-1 unperturbed neurons assumed to be oscillating synchronously (*Lemma*). We are interested in the stability of synchrony of the network, where, following the perturbation of a single neuron, the two resulting oscillators synchronize as a single network of N oscillators. To obtain a criterion that describes the stability of synchrony we first define synchrony as a steady-state equilibrium for a discrete linear map based on perturbation. The stability would then be determined using the eigen value of the discrete map. Figure 3A shows the intervals that we will use to define the discrete

map. Using the definitions of stimulus interval and response interval, the two main constraints that are used to construct the discrete map are:

$$ts_{N-1}[n] + tr_{N-1}[n] + ts_{N-1}[n+1] = \delta + tr_1[n] + \delta$$

$$ts_1[n] + tr_1[n] + ts_1[n+1] = \delta + tr_{N-1}[n] + \delta$$

At synchrony, the steady-state intervals (if steady-state exists) would be:

$$ts_{N-1}[\infty] + tr_{N-1}[\infty] + ts_{N-1}[\infty] = 2\delta + tr_1[\infty]$$

$$ts_1[\infty] + tr_1[\infty] + ts_1[\infty] = 2\delta + tr_{N-1}[\infty]$$

Note that the two constraints have common terms and so we would get a one-dimensional discrete map.

We also define the phase in the nth cycle as a perturbation from the fixed point φ^*: $\varphi[n] = \varphi^* + \Delta\varphi[n]$. Using the definition of the response interval in terms of the PRC and linearizing the PRC around the fixed point at the locking phase as $f(\varphi[n]) = f(\varphi^*) + f'(\varphi^*)\Delta\varphi[n]$. Continuing with substitutions along these lines we get a one-dimensional discrete map as:

$$\Delta\varphi_1[n+1] = \left(1 - f'_{1,N-1}(\varphi_1^*) - f'_{N-1,1}(\varphi_{N-1}^*)\right)\Delta\varphi_1[n]$$

where $f'_{i,j}$ are the slopes of the respective PRCs. The detailed derivation of this map can be found in Appendix A.

For synchrony as a fixed point of this map to be stable, the perturbation must decay $\Delta\varphi_1[n+1] \to 0$ as n → ∞. To that end, the eigenvalue for the map $\lambda =$

$\left(1 - f'_{1,N-1}(\varphi_1^*) - f'_{N-1,1}(\varphi_{N-1}^*)\right)$ must have an absolute value less than 1. Since the oscillators are all identical and we know the intrinsic period of a single oscillator, we can obtain the steady-state phases for each case. Also, since the PRCs are simulated for each oscillator are computed through simulations, the PRC for the self-connected unperturbed network $f_{N-1,1}$ becomes a function of the synaptic delay. Thus, we get the stability criterion:

Eq. 1

$$\left|1 - f'_{1,N-1}\left(\frac{\delta}{P_i}\right) - f'_{N-1,1,\delta}\left(\frac{\delta}{P_i\left(1 + f_{1,N-2}\left(\frac{\delta}{P_i}\right)\right)}\right)\right| < 1$$

The above discussion can be summarized as the following theorem:

Theorem 1: *Stability of Synchrony in a Single Cluster*

If a network of N identical neurons with synaptic delays and each receiving N-1 inputs achieves synchrony as a steady-state phase-locking mode in the case of a single-neuron perturbation, then the synchrony is stable if the following criterion holds:

Eq. 1 $$\left|1 - f'_{1,N-1}\left(\frac{\delta}{P_i}\right) - f'_{N-1,1,\delta}\left(\frac{\delta}{P_i\left(1+f_{1,N-2}\left(\frac{\delta}{P_i}\right)\right)}\right)\right| < 1$$

Figure 4 addresses an all-to-all network of 25 identical Via model inhibitory neurons as described in the Methods. This network was chosen to correspond loosely to the sparsely

connected homogeneous network from [15]. Delays were sampled at intervals of 5 percent of the period both in the emulator and to apply the stability criterion in Eq. 1.

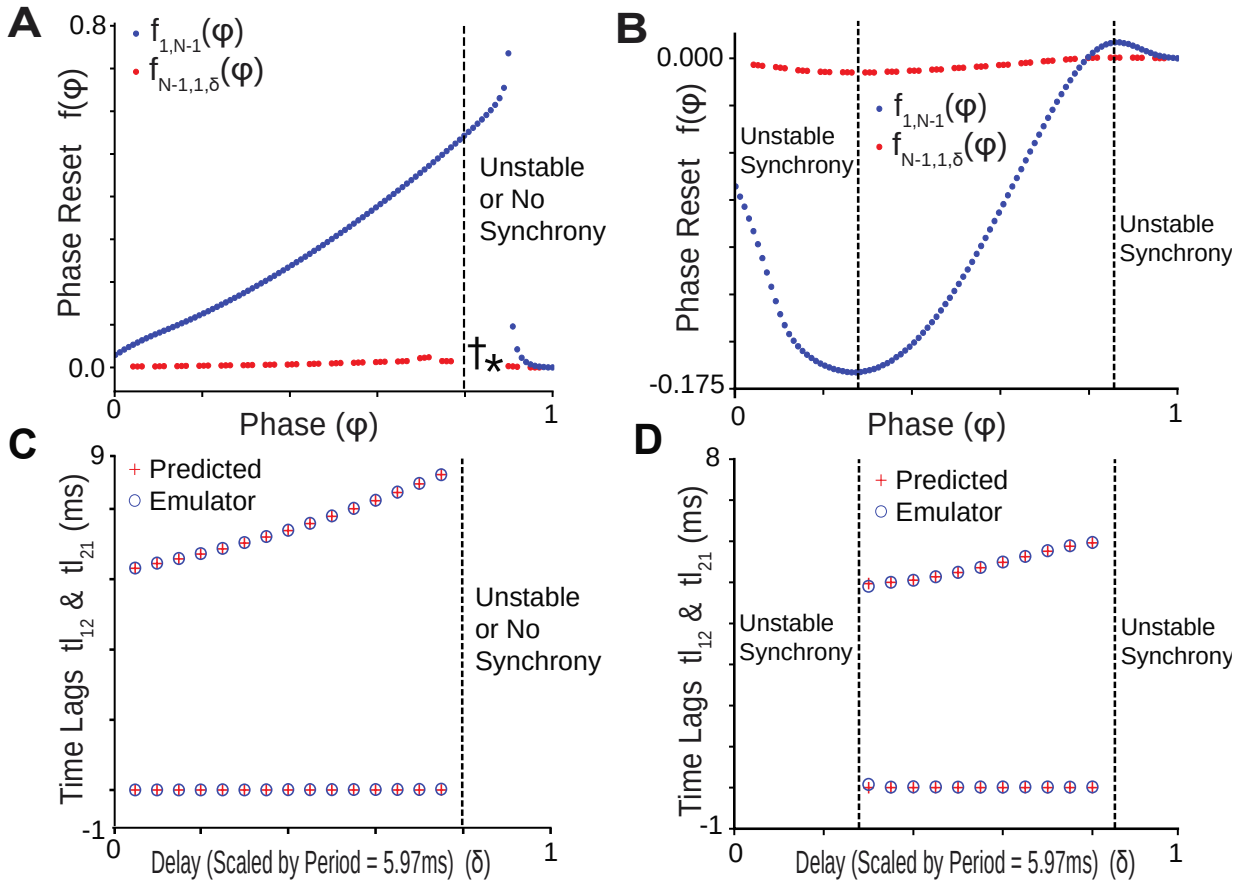

Fig. 4. Predicted and Observed Periods for Global Synchrony. A. PRC of a single oscillator (blue) in response to a population spike in all other oscillators with E_{GABA} = -75 mV and of a self-connected oscillator representing the rest of the network. The set of points depicted in red color corresponds to three points from each PRC $f_{1,N-1,\delta}(\varphi)$ parameterized by the delay (equal to the locking phase) to give the slope at each delay δ. * and † indicate the special cases with delays 4.8 ms and 5.1 ms, discussed in the case of existence of self-locking. B. Same as A with shunting reversal potential. C and D. Plots of predicted versus observed time-lags in cases where synchrony was predicted to be stable using Eq.1.

Figs. 4A (E_{GABA} = -75 mV) and 4B (E_{GABA} = -55 mV) depict the PRCs of both oscillators in Fig. 3B due to perturbation by each other (Fig. 3B). The curve in blue represents the PRC of the single perturbed neuron due to the self-connected cluster $f_{1,N-1}(\varphi)$ representing the rest of he network. Since the PRCs for the self-connected oscillator are

parametrized by the delay, the sets of points depicted in red color correspond to three points sampled around the locking phase (equal to the normalized feedback delay) in order to calculate the slope of the PRC $f_{1,N-1,\delta}(\varphi)$ for each delay δ.

Fig. 4C and 4D show that the time lags between the firing of oscillators predicted by the criterion Eq.1 match with the time lags observed from the emulator simulations when synchrony is predicted. To the right of the dashed line in Fig. 4A and C, we have not used the emulator map to test due one of the following reasons:

1. *Unstable synchrony predicted:* For the cases with delays 5.4 ms and 5.7 m, the eigen value of the discrete map calculated using Eq. 1 is greater than 1, indicating that the synchrony, if exists, is unstable. This means that unless the oscillators are initialized to be already in synchrony, they would not fire in synchrony and any perturbation would disrupt their synchrony. The reason is that the respective slopes of PRCs are negative. Therefore, although the respective PRCs $f_{1,N-1,\delta}(\varphi)$ have been calculated and plotted (red point-traces in Fig 4C), the predicted and observed periods are not plotted since synchrony is not observed when tested in the emulator.
2. *Phase-locking did not exist:* For the case with delay 5.1 ms, we saw from the lemma that the self-connected oscillator would not be able to phase-lock. The discontinuity in the second-order resetting is the cause for this situation. Periodicity of spiking was not observed and as a result the PRC $f_{1,N-1,\delta}(\varphi)$ could not be measured for this case. Therefore, the criterion in Eq. 1 is not applicable to this case. This is denoted by ***** in Fig. 4A.

3. Phase-locking was predicted to exist, but periodicity was not observed: For the case with delay 4.8 ms, we saw that even though the existence of self-locking was predicted, periodicity was not observed in simulations. As a result, here too the PRC $f_{1,N-1,\delta}(\varphi)$ could not be measured and therefore the criterion in Eq. 1 is not applicable to this case. This is denoted by a dagger **†** in Fig. 4A.

In case of the figures 4B and 4D, the existence of self-locking was established for all delays (data not shown). The dashed-line dividers in figures 4B and 4D only indicate the delays where the stability criterion given by Eq. 1 has an eigen value greater than 1. The reason for this is the negative slope in PRCs.

Although both reversal potential values are physiologically plausible [31], they result in vastly different phase resetting curves. In contrast to the hyperpolarizing case, for shunting inhibition there is both a lower and an upper bound on the delays that support stable synchrony because there are two regions of negative slope in the PRC, which make synchrony unstable. In the regions that did not support stable synchrony, we did not observe synchrony when tested in the emulator.

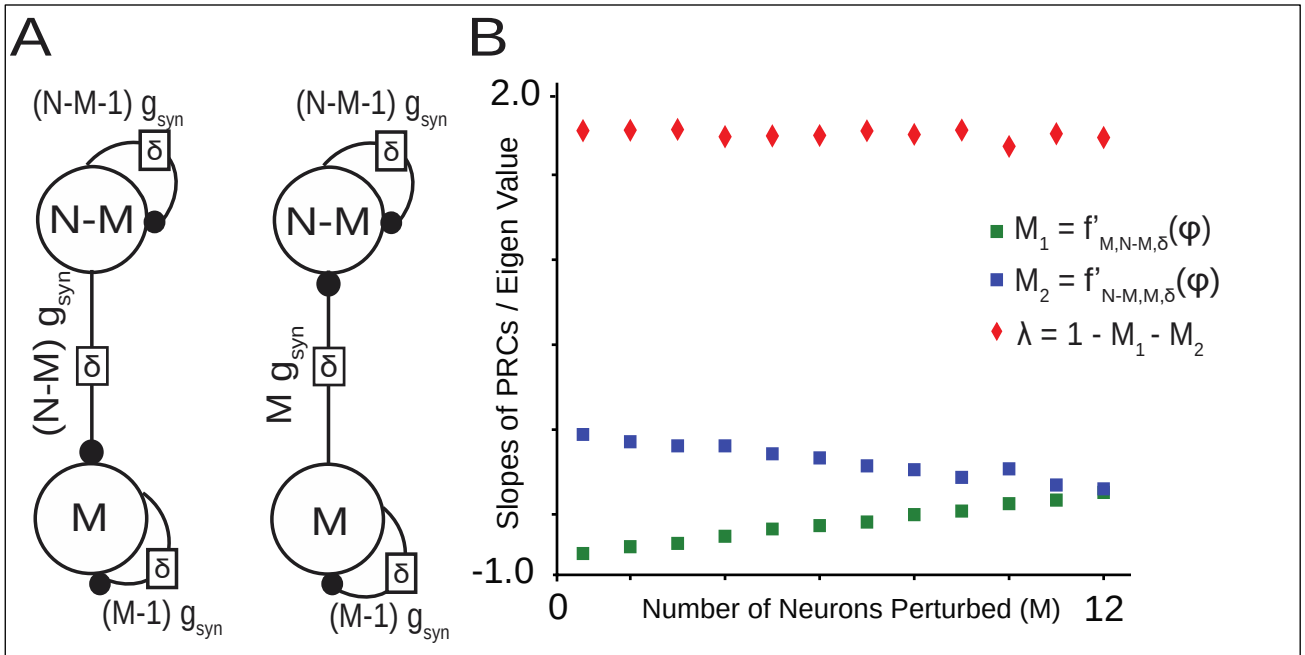

Fig 5. Multiple-Neuron Perturbation and Eigen Values. A. Depiction of the two oscillators when M neurons are perturbed. Both the clusters are assumed to receive delayed synchronous feedback from themselves without autapses. B. For a fixed delay of 0.3 ms in the example where shunting inhibition is used, the figure shows slopes and eigenvalues plotted against the number of neurons perturbed from the network (M).

3.4 Extension of the results for perturbation of more than one neuron:

Instead of perturbing just a single neuron, if we perturb more than one, the second oscillator becomes another self-connected cluster. Figure 5A shows the two oscillators and their connections when M neurons are perturbed from a cluster of N neurons. The unperturbed cluster contains N-M neurons with N-M-1 self-connections, whereas the perturbed cluster with M neurons receives M-1 inputs due to self-connections. Extending Eq.1 to the perturbation for M neurons ($1 \leq M \leq N$), we get a generalized criterion:

Eq. 2

$$\left| 1 - f'_{M,N-M,\delta}\left(\frac{\delta}{P_i\left(1 + f_{1,M-1}(\delta/P_i)\right)}\right) - f'_{N-M,M,\delta}\left(\frac{\delta}{P_i\left(1 + f_{1,N-M-1}(\delta/P_i)\right)}\right)\right| < 1$$

From the equation above, we see that in the multiple-neuron perturbation case, the PRCs of both oscillators are functions of the delay. Further, we wanted to check if the assumption that the single neuron perturbation from the network is the most destabilizing (Canavier and Achuthan, 2010) holds even in the presence of delays and self-connections. To that end, we took the specific case from the model (considered above) with shunting inhibition and a delay of 0.3 ms which had the greatest eigenvalue greater than 1 for a single neuron perturbation case. To this, we varied the number of perturbed

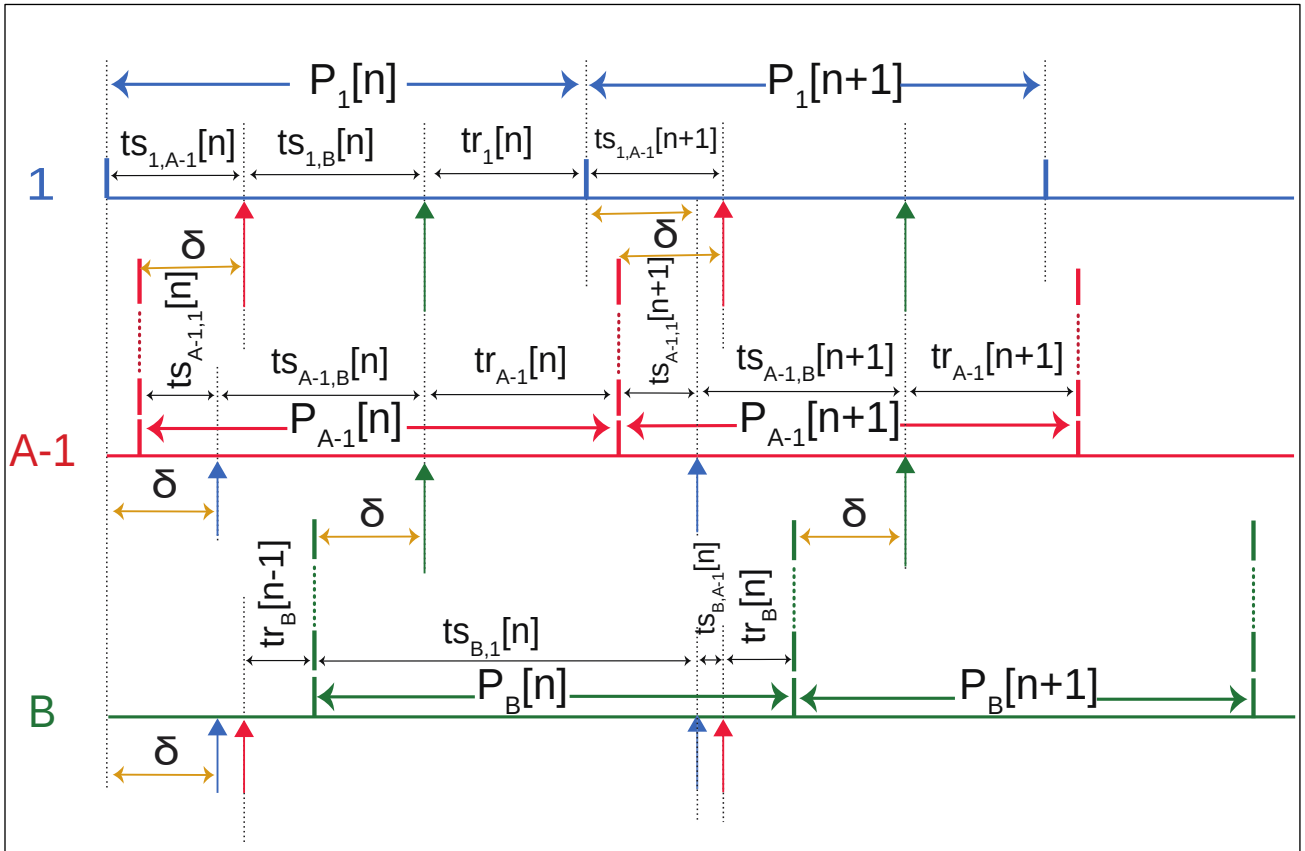

Fig 6. Firing intervals for perturbation of Two Cluster Network. Schematic firing pattern in which a single neuron is perturbed from one cluster in the two-cluster case. These intervals are used to derive the discrete map through which a stability criterion of the two-cluster solution is established.

neurons from the network of 25 between M = 2 and M = 12. In each case, we used Eq. 2 to obtain the eigen value of the discrete map that suggests stability. The plot of slopes and eigenvalues in each case can be found in Figure 5B. From the empirical observations,

we see that for all perturbations including 1 till 12, the eigenvalues do not drastically change, indicating that for this case, the perturbing any number of neurons could determine the stability of synchrony of the all-to-all network.

3.5 Extension of the results for alternating firing of two nonidentical clusters without delay to include delays:

Previously, we showed how an alternating firing pattern between two clusters, A and B, can enforce synchrony within each cluster, even if neither cluster is capable of synchronizing in isolation [32]. The key is the multiplicative nature of the factors that scale the perturbation in separate intervals. We assume once again that the perturbation of a single neuron from a fully synchronized cluster is the most destabilizing perturbations (one such perturbation is illustrated in Fig. 6.) A two-cluster mode cannot be presumed to exist but must satisfy the existence criteria determined by the firing intervals in Fig. 5. The existence criterion is simply that [12] $tr_A[\infty]+2\delta = ts_B[\infty]$ and $tr_B[\infty]+2\delta = ts_A[\infty]$, where the stimulus and response intervals in the steady 1:1 phase locked mode are determined by the phase response curves.

Unlike global synchrony, this system cannot be reduced to a single coupled map. Instead, due to the presence of three oscillators, we get a two-dimensional discrete map leading to two eigen values. Based on figure 6, like the global synchrony case, the constraints that lead to the map are:

$$2\delta + tr_{A-1}[n] = ts_{B,1}[n] + ts_{B,A-1}[n] \qquad (1)$$

$$ts_{B,1}[n] = \delta + tr_{A-1}[n] + ts_{A-1,1}[n+1] \qquad (2)$$

$$ts_{A-1,B}[n+1] = ts_{B,A-1}[n] + tr_B[n] + \delta \quad (3)$$

$$ts_{1,B}[n+1] = tr_B[n] + \delta \quad (4)$$

$$ts_{B,1}[n] = 2\delta + tr_1[n] \quad (5)$$

$$ts_{1,A-1}[n+1] = \delta + ts_{B,A-1}[n] \quad (6)$$

The derivation of the 2-dimensional discrete map and the discussion leading up to the eigen values can be found in Appendix -B. Based on the two eigenvalues, we get two criteria. For a perturbation of a single neuron from cluster A (illustrated in Fig. 4), one criterion is

Eq. 3 $$-1 < (1 - f'_{A,B}(\varphi_A))\left(1 - f'_{1,A-1}\left(\frac{\delta}{P_1}\right) - f'_{A-1,1}\left(\frac{\delta}{P_{A-1}}\right)\right) < 1$$

in which the large parentheses enclose the within cluster synchrony term for cluster A and is scaled by the term representing forcing of cluster A by cluster B: $1 - f'_{A,B}(\varphi_A)$.

Another criterion, consisting solely of between cluster terms is

Eq. 4 $$-1 < (1 - f'_{A,B}(\varphi_A))(1 - f'_{B,A-1}(\varphi_B))(1 - f'_{B,1}(\varphi_B)) < 1$$

To test the predictions in the two-cluster case, we considered the inhibitory neurons used in the global synchrony case as one cluster, and the RTM model of excitatory neurons described in methods as the second cluster. Unlike the network of inhibitory neurons, the excitatory neurons are not assumed to be self-connected, as is the case for excitatory neurons in layer 2/3 entorhinal cortex [33]. Therefore, we consider the whole cluster of excitatory neurons as a single oscillator that is firing in synchrony (denoted by B in Fig.

6). Since this testing is essentially meant to understand the influence of the second cluster on the existing cluster that cannot synchronize by itself, we considered the inhibitory neurons with shunting reversal potential at a delay of 0.3ms, which denotes the most destabilizing case for the cluster of inhibitory neurons. Figures 7A1 shows the output from the emulator depicting how the oscillators do not synchronize when a single neuron is perturbed from the inhibitory cluster at the aforementioned delay. The arrows in the figure 7A2 of PRCs show how the negative slopes of the PRCs influence the eigenvalue (Eq.1) to be 1.75 (greater than 1 denotes unstable synchrony).

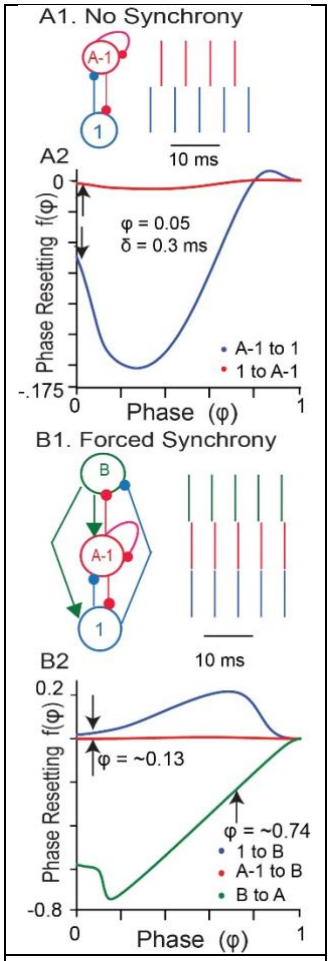

Figure 7. **Two cluster synchrony A**. A self-connected cluster of A neurons (red) cannot synchronize itself when one neuron (blue) is perturbed because the slopes of the PRCs at the locking point are negative. **B**. Mutual coupling to a population of excitatory cells (green) enforces synchrony.

However, when we add the cluster of excitatory neurons, from the emulator results shown in figure 7B1, we see that the two oscillators of the inhibitory cluster fire synchronously. The PRCs as shown in figure 7B2 in fact show that the phase at which the excitatory input reaches the inhibitory neurons is highly stabilizing (with its slope almost 1). Thus, from Eq.3, we see that the forcing term dominates the effect of the single-neuron perturbation within the cluster.

4. Discussion

4.1 Generality: The results presented herein generalize to any system of pulse-coupled oscillators with delays including synchronization of fireflies [5], cardiac pacemaker cells

[34–36], circadian rhythms [24] and in the engineering application of pulse-coupled sensor networks [37–40].

4.2 Role of Delays in Neuronal Networks: In the nervous system, there is always a delay between an action potential in the pre-synaptic neuron and the postsynaptic potential observed at chemical synapses, due to the time required for an action potential to propagate from the axon initial segment to the axonal terminal and for the neurotransmitter to diffuse across the synaptic cleft and bind to the post-synaptic ionotropic receptors [41]. Delays in synchronization of inhibitory networks have previously been shown to promote synchrony [42,43]. The innovation herein is to use delayed self-connections to represent breaking the network into smaller clusters to rigorously determine the stability of one and two-cluster synchrony.

4.3 *Discontinuity in the PRC:* Discontinuous PRCs have been previously observed [44,45]. Although the dynamical system representing the oscillator is continuous, the use of events such as the action potential to define the windows within which phase resetting occurs allows for discontinuities in the PRC. For example, the discontinuity at late phases in Fig. 1B occurs at the phase at which the perturbation cannot hyperpolarize the neuron sufficiently to stop the action potential from occurring, and the bulk of its effect occurs in the next oscillation cycle, resulting in second order resetting instead. The curves for both first and second order resetting are discontinuous. Basically, the PRC function become discontinuous for inputs that arrive at a later phase. We can observe that for such inputs, the second order resetting is greater than the first order resetting. However, this increase in second order resetting also is after a discontinuity. In fact, this discontinuity accounts for the non-existence of phase-locking of self-connected oscillator when the inputs arrive

after a delay of 5.1 ms. As a result the slope of the PRC becomes undefined at those points and so phase locking does not exist at phases that fall in the discontinuity. However, it is clear that this discontinuity is highly repelling [43,46].

4.4 Higher-Order Phase Resetting: In the criterion for existence of phase-locking in a self-connected oscillator, we included second order resetting into the stimulus interval of the first cycle following the perturbation [11]. Otherwise, here we ignore the second-order resetting, or any other higher order resetting. It does not seem possible to incorporate third and higher order resetting into our simple pulsatile coupling framework, which is a limitation our methods. Others [47] have considered the case in which an oscillator does not return to its original limit cycle by the time the next input is received .

4.5 Perturbation of a single neuron from a cluster versus multiple neurons: From the empirical results in Fig. 5 for the case of all-to-all network synchrony, we saw that the eigenvalues of the discrete map did not depend strongly on the the number of neurons perturbed from global synchrony. In order to guarantee stability, in some small neighborhood around the fixed point of the map, synchrony must be robust to all possible perturbations. Therefore, if any specific perturbation is predicted to grow rather than decay, synchrony is unstable. However, the simplest perturbation (Eq. 1), that of a single neuron from a stable cluster, may provide useful insights regarding whether a system can synchronize, although technically Eq. 2 must also be considered.

4.6 Applications to Neural Oscillations: There are numerous examples in the literature about how populations of excitatory neurons can synchronize themselves via mutual

coupling with populations of inhibitory neurons [48–51] in a type of brain rhythm called pyramidal interneuronal network gamma (PING). Many of these mechanisms assume that the excitatory neurons are driven above threshold (mean driven) but inhibitory neurons are quiescent in the absence of excitation via their local excitatory neuron partners [52], whereas other assume that both populations are in the fluctuation driven regime below threshold [53–55]. We propose a third mechanism by which the excitatory cells can synchronize tonically firing interneurons that cannot synchronize themselves, as in Fig. 7. During theta oscillations, the firing rate of fast spiking interneuron increases [56], thus it is possible that interneurons are in the mean driven regime during theta nested gamma. In optogenetically-driven theta-nested gamma in a slice preparation [57], the interneurons are indeed tonically active during the peak of theta with excitation blocked. In that study, the interneurons only synchronized with excitation intact. Under similar optogenetic drive, we have observed some gamma synchrony in the absence of excitation; however, recruiting excitatory cells into optogenetically-driven theta nested gamma [58] increases gamma power, perhaps by a similar mechanism as in Fig. 7.

5. Conclusions

We extended our previous criteria for stability of one and two cluster synchrony in networks of pulse-coupled oscillators to include conduction delays shorter than the intrinsic period using self-connected oscillators to represent perturbed clusters of oscillators. We also showed that second order resetting can prevent the existence of self-locked synchrony, which is a prerequisite for the application of the stability criteria we present.

Acknowledgements

This work was funded by NIH R01NS054281 to CCC. The funding agency had no role in the collection, analysis and interpretation of data, in the writing of the report or in the decision to submit the article for publication.

Conflict of Interest

The authors declare no conflict of interest.

References

[1] G.B. Ermentrout, C.C. Chow, Modeling neural oscillations, Physiol. Behav. 77 (2002) 629–633.

[2] F. Núñez, Y. Wang, A.R. Teel, F.J. Doyle, Synchronization of pulse-coupled oscillators to a global pacemaker, Syst. Control Lett. 88 (2016) 75–80. https://doi.org/10.1016/j.sysconle.2015.11.007.

[3] G.B. Ermentrout, N. Kopell, Multiple pulse interactions and averaging in systems of coupled neural oscillators, J. Math. Biol. 29 (1991) 195–217. https://doi.org/10.1007/BF00160535.

[4] J. Rinzel, G.B. Ermentrout, Analysis of neural excitability and oscillations, Methods Neuronal Model. Ions Netw. 2 (1998) 251–291.

[5] R.E. Mirollo, S.H. Strogatz, Synchronization of Pulse-Coupled Biological Oscillators, SIAM J. Appl. Math. 50 (1990) 1645–1662. https://doi.org/10.1137/0150098.

[6] C.C. Canavier, S. Achuthan, Pulse coupled oscillators and the phase resetting curve, Math. Biosci. 226 (2010) 77–96. https://doi.org/10.1016/j.mbs.2010.05.001.

[7] N. Brunel, D. Hansel, How Noise Affects the Synchronization Properties of Recurrent Networks of Inhibitory Neurons, Neural Comput. 18 (2006) 1066–1110.

[8] C.D. Acker, N. Kopell, J.A. White, Synchronization of strongly coupled excitatory neurons: relating network behavior to biophysics, J. Comput. Neurosci. 15 (2003) 71–90. https://doi.org/10.1023/a:1024474819512.

[9] P. Malerba, N. Kopell, Phase resetting reduces theta–gamma rhythmic interaction to a one-dimensional map, J. Math. Biol. 66 (2013) 1361–1386. https://doi.org/10.1007/s00285-012-0534-9.

[10] D.H. Perkel, J.H. Schulman, T.H. Bullock, G.P. Moore, J.P. Segundo, PACEMAKER NEURONS: EFFECTS OF REGULARLY SPACED SYNAPTIC INPUT, Science. 145 (1964) 61–63. https://doi.org/10.1126/science.145.3627.61.

[11] S. Achuthan, C.C. Canavier, Phase-Resetting Curves Determine Synchronization, Phase Locking, and Clustering in Networks of Neural Oscillators, J. Neurosci. 29 (2009) 5218–5233. https://doi.org/10.1523/JNEUROSCI.0426-09.2009.

[12] M.M. Woodman, C.C. Canavier, Effects of conduction delays on the existence and stability of one to one phase locking between two pulse-coupled oscillators, J. Comput. Neurosci. 31 (2011) 401–418. https://doi.org/10.1007/s10827-011-0315-2.
[13] R.O. Dror, C.C. Canavier, R.J. Butera, J.W. Clark, J.H. Byrne, A mathematical criterion based on phase response curves for stability in a ring of coupled oscillators, Biol. Cybern. 80 (1999) 11–23. https://doi.org/10.1007/s004220050501.
[14] S.A. Oprisan, A.A. Prinz, C.C. Canavier, Phase resetting and phase locking in hybrid circuits of one model and one biological neuron, Biophys. J. 87 (2004) 2283–2298. https://doi.org/10.1529/biophysj.104.046193.
[15] G. Via, R. Baravalle, F.R. Fernandez, J.A. White, C.C. Canavier, Interneuronal network model of theta-nested fast oscillations predicts differential effects of heterogeneity, gap junctions and short term depression for hyperpolarizing versus shunting inhibition, PLOS Comput. Biol. 18 (2022) e1010094. https://doi.org/10.1371/journal.pcbi.1010094.
[16] A.L. Hodgkin, The local electric changes associated with repetitive action in a non-medullated axon, J. Physiol. 107 (1948) 165–181.
[17] A.L. Hodgkin, A.F. Huxley, A quantitative description of membrane current and its application to conduction and excitation in nerve, J. Physiol. 117 (1952) 500–544.
[18] D.A. Baxter, C.C. Canavier, J.H. Byrne, CHAPTER 7 - Dynamical Properties of Excitable Membranes, in: J.H. Byrne, J.L. Roberts (Eds.), Mol. Netw., Academic Press, Burlington, 2004: pp. 161–196. https://doi.org/10.1016/B978-012148660-0/50008-1.
[19] A. Erisir, D. Lau, B. Rudy, C.S. Leonard, Function of Specific K+ Channels in Sustained High-Frequency Firing of Fast-Spiking Neocortical Interneurons, J. Neurophysiol. 82 (1999) 2476–2489. https://doi.org/10.1152/jn.1999.82.5.2476.
[20] D. Golomb, K. Donner, L. Shacham, D. Shlosberg, Y. Amitai, D. Hansel, Mechanisms of Firing Patterns in Fast-Spiking Cortical Interneurons, PLOS Comput. Biol. 3 (2007) e156. https://doi.org/10.1371/journal.pcbi.0030156.
[21] F.R. Fernandez, G. Via, C.C. Canavier, J.A. White, Kinetics and Connectivity Properties of Parvalbumin- and Somatostatin-Positive Inhibition in Layer 2/3 Medial Entorhinal Cortex, eNeuro. 9 (2022). https://doi.org/10.1523/ENEURO.0441-21.2022.
[22] R.D. Traub, R. Miles, Neuronal Networks of the Hippocampus, Cambridge University Press, 1991.
[23] C. Börgers, Three Simple Models of Neurons in Rodent Brains, in: C. Börgers (Ed.), Introd. Model. Neuronal Dyn., Springer International Publishing, Cham, 2017: pp. 31–37. https://doi.org/10.1007/978-3-319-51171-9_5.
[24] A.T. Winfree, The Geometry of Biological Time, Springer London, Limited, 1990.
[25] V.V. Klinshov, V.I. Nekorkin, The map with no predetermined firing order for the network of oscillators with time-delayed pulsatile coupling, Commun. Nonlinear Sci. Numer. Simul. 18 (2013) 973–977. https://doi.org/10.1016/j.cnsns.2012.09.012.
[26] R. Goebel, R.G. Sanfelice, A.R. Teel, Hybrid Dynamical Systems: Modeling, Stability, and Robustness, Princeton University Press, 2012. http://www.barnesandnoble.com/w/hybrid-dynamical-systems-rafal-goebel/1120733646 (accessed April 1, 2015).

[27] J.A. White, C.C. Chow, J. Ritt, C. Soto-Treviño, N. Kopell, Synchronization and oscillatory dynamics in heterogeneous, mutually inhibited neurons, J. Comput. Neurosci. 5 (1998) 5–16.
[28] J. Foss, J. Milton, Multistability in recurrent neural loops arising from delay, J. Neurophysiol. 84 (2000) 975–985. https://doi.org/10.1152/jn.2000.84.2.975.
[29] M. Golubitsky, I. Stewart, Nonlinear dynamics of networks: the groupoid formalism, Bull. Am. Math. Soc. 43 (2006) 305–365. https://doi.org/10.1090/S0273-0979-06-01108-6.
[30] C.C. Canavier, S. Achuthan, History of the application of the phase resetting curve to neurons coupled in a pulsatile manner, in: N.W. Schultheiss, A.A. Prinz, R.J. Butera (Eds.), Phase Response Curves Neurosci., Springer New York, New York, NY, 2012: pp. 73–91. http://link.springer.com/10.1007/978-1-4614-0739-3 (accessed September 25, 2015).
[31] Y. Otsu, F. Donneger, E.J. Schwartz, J.C. Poncer, Cation–chloride cotransporters and the polarity of GABA signalling in mouse hippocampal parvalbumin interneurons, J. Physiol. 598 (2020) 1865–1880. https://doi.org/10.1113/JP279221.
[32] L. Chandrasekaran, S. Achuthan, C. Canavier, Stability of two cluster solutions in pulse coupled networks of neural oscillators, J. Comput. Neurosci. 30 (2011) 427–445.
[33] J.J. Couey, A. Witoelar, S.-J. Zhang, K. Zheng, J. Ye, B. Dunn, R. Czajkowski, M.-B. Moser, E.I. Moser, Y. Roudi, M.P. Witter, Recurrent inhibitory circuitry as a mechanism for grid formation, Nat. Neurosci. 16 (2013) 318–324. https://doi.org/10.1038/nn.3310.
[34] C.S. Peskin, Mathematical aspects of heart physiology, Courant Institute of Mathematical Sciences, New York University, 1975.
[35] M.R. Guevara, A. Shrier, L. Glass, Phase resetting of spontaneously beating embryonic ventricular heart cell aggregates, Am. J. Physiol. 251 (1986) H1298-1305. https://doi.org/10.1152/ajpheart.1986.251.6.H1298.
[36] M.R. Guevara, L. Glass, Phase locking, period doubling bifurcations and chaos in a mathematical model of a periodically driven oscillator: a theory for the entrainment of biological oscillators and the generation of cardiac dysrhythmias, J. Math. Biol. 14 (1982) 1–23. https://doi.org/10.1007/BF02154750.
[37] J. Nishimura, E.J. Friedman, Robust convergence in pulse-coupled oscillators with delays, Phys. Rev. Lett. 106 (2011) 194101. https://doi.org/10.1103/PhysRevLett.106.194101.
[38] Y. Wang, F. Nunez, F.J. Doyle, Statistical analysis of the pulse-coupled synchronization strategy for wireless sensor networks, IEEE Trans. Signal Process. 61 (2013) 5193–5204. https://doi.org/10.1109/TSP.2013.2275511.
[39] Y. Wang, K. Mosalakanti, F. Núñez, S. Deligeorges, F.J. Doyle, A kernel module for pulse-coupled time synchronization of sensor networks, Comput. Netw. 127 (2017) 161–172. https://doi.org/10.1016/j.comnet.2017.08.009.
[40] F. Núñez, Y. Wang, A.R. Teel, F.J. Doyle, Synchronization of pulse-coupled oscillators to a global pacemaker, Syst. Control Lett. 88 (2016) 75–80. https://doi.org/10.1016/j.sysconle.2015.11.007.
[41] E.R. Kandel, J.H. Schwartz, T.M. Jessell, Principles of Neural Science, 4 edition, McGraw-Hill Medical, New York, 2000.

[42] N. Roohi, A. Valizadeh, Role of Interaction Delays in the Synchronization of Inhibitory Networks, Neural Comput. 34 (2022) 1425–1447. https://doi.org/10.1162/neco_a_01500.
[43] R.A. Tikidji-Hamburyan, C.A. Leonik, C.C. Canavier, Phase Response Theory Explains Cluster Formation in Sparsely but Strongly Connected Inhibitory Neural Networks and Effects of Jitter due to Sparse Connectivity, J. Neurophysiol. (2019). https://doi.org/10.1152/jn.00728.2018.
[44] L. Glass, A.T. Winfree, Discontinuities in phase-resetting experiments, Am. J. Physiol. 246 (1984) R251-258.
[45] T. Krogh-Madsen, L. Glass, E.J. Doedel, M.R. Guevara, Apparent discontinuities in the phase-resetting response of cardiac pacemakers, J. Theor. Biol. 230 (2004) 499–519. https://doi.org/10.1016/j.jtbi.2004.03.027.
[46] C.C. Canavier, R.A. Tikidji-Hamburyan, Globally attracting synchrony in a network of oscillators with all-to-all inhibitory pulse coupling, Phys. Rev. E. 95 (2017) 032215. https://doi.org/10.1103/PhysRevE.95.032215.
[47] V. Klinshov, S. Yanchuk, A. Stephan, V. Nekorkin, Phase response function for oscillators with strong forcing or coupling, Europhys. Lett. 118 (2017) 50006. https://doi.org/10.1209/0295-5075/118/50006.
[48] M.A. Whittington, R.D. Traub, J.G. Jefferys, Synchronized oscillations in interneuron networks driven by metabotropic glutamate receptor activation, Nature. 373 (1995) 612–615.
[49] A. Fisahn, F.G. Pike, E.H. Buhl, O. Paulsen, Cholinergic induction of network oscillations at 40 Hz in the hippocampus in vitro, Nature. 394 (1998) 186–189. https://doi.org/10.1038/28179.
[50] M. Bartos, I. Vida, P. Jonas, Synaptic mechanisms of synchronized gamma oscillations in inhibitory interneuron networks, Nat. Rev. Neurosci. 8 (2007) 45–56. https://doi.org/10.1038/nrn2044.
[51] P. Tiesinga, T.J. Sejnowski, Cortical enlightenment: are attentional gamma oscillations driven by ING or PING?, Neuron. 63 (2009) 727–732. https://doi.org/10.1016/j.neuron.2009.09.009.
[52] C. Börgers, N. Kopell, Synchronization in networks of excitatory and inhibitory neurons with sparse, random connectivity, Neural Comput. 15 (2003) 509–538. https://doi.org/10.1162/089976603321192059.
[53] N. Brunel, X.-J. Wang, What determines the frequency of fast network oscillations with irregular neural discharges? I. Synaptic dynamics and excitation-inhibition balance, J. Neurophysiol. 90 (2003) 415–430. https://doi.org/10.1152/jn.01095.2002.
[54] C. Geisler, N. Brunel, X.-J. Wang, Contributions of intrinsic membrane dynamics to fast network oscillations with irregular neuronal discharges, J. Neurophysiol. 94 (2005) 4344–4361. https://doi.org/10.1152/jn.00510.2004.
[55] G. Buzsáki, X.-J. Wang, Mechanisms of gamma oscillations, Annu. Rev. Neurosci. 35 (2012) 203–225. https://doi.org/10.1146/annurev-neuro-062111-150444.
[56] D. Lapray, B. Lasztoczi, M. Lagler, T.J. Viney, L. Katona, O. Valenti, K. Hartwich, Z. Borhegyi, P. Somogyi, T. Klausberger, Behavior-dependent specialization of identified hippocampal interneurons, Nat. Neurosci. 15 (2012) 1265–1271. https://doi.org/10.1038/nn.3176.

[57] H. Pastoll, L. Solanka, M.C.W. van Rossum, M.F. Nolan, Feedback inhibition enables θ-nested γ oscillations and grid firing fields, Neuron. 77 (2013) 141–154. https://doi.org/10.1016/j.neuron.2012.11.032.

[58] B. Williams, F.R. Fernandez, C.C. Canavier, J.A. White, Synaptic mechanisms of theta-nested gamma oscillations in the medial entorhinal cortex, (2023). https://www.abstractsonline.com/pp8/#!/10892/presentation/33250 (accessed December 1, 2023).

Appendix A: Derivation for Stability of Synchrony in an All-to-All Network

Let P_1 and P_{N-1} be the intrinsic periods of the two pulse-coupled oscillators. Figure 3A and 3B describe the nature, connections and intervals of both the oscillators. Based on the figure, the cluster with $N-1$ neurons is treated as a single oscillator labelled $N-1$ as it is assumed to be oscillating in synchrony, in which case, P_{N-1} denotes the network period at which each neuron oscillates. A necessary condition for stability of synchrony in a network of N oscillators is that it be robust to perturbing even one of them. Perturbing a single neuron from a synchronous cluster introduces the perturbation into all affected intervals (Figure 3B). The goal is to define a discrete linear map and arrive at the stability criterion based on the eigen values of this map.

As defined earlier, $ts_i[k]$ stands for the *Stimulus Interval* of the ith oscillator in its kth cycle. $tr_i[k]$ stands for the *Response Interval* of the ith oscillator in its kth cycle. The *Phase* of the oscillator i in its kth cycle is defined as

$$\varphi_i[k] = \frac{ts_i[k]}{P_i}$$

Thus, from the definitions given earlier, the *Stimulus Interval* of the ith oscillator in its kth cycle can be expanded as:

$$ts_i[k] = P_i\varphi_i[k]$$

and, the *Response Interval* of the ith oscillator in its kth cycle as

$$tr_i[k] = P_i(1 - \varphi_i[k] - f_{i,j}\,(\varphi_i[k])$$

where $f_{i,j}(\varphi_i[k])$ is the *Phase Resetting Curve* of the ith oscillator due to the input from j^{th} oscillator in its kth cycle. We ignore second order resetting for this criterion. Figure 3A shows schematically the perturbation and the intervals defined for each of the oscillators in their n^{th} cycle.

From the figure 3A above, the two main constraints that relate the intervals of the two oscillators can be written as

$$ts_{N-1}[n] + tr_{N-1}[n] + ts_{N-1}[n+1] = \delta + tr_1[n] + \delta \quad (1)$$

$$ts_1[n] + tr_1[n] + ts_1[n+1] = \delta + tr_{N-1}[n] + \delta \quad (2)$$

Further, based on the figure, we get an additional constraint given by:

$$ts_{N-1}[n] + tr_{N-1}[n] + \delta = \delta + tr_1[n] + ts_1[n+1] \quad (3)$$

Simplifying the above constraint (3),

$$ts_{N-1}[n] + tr_{N-1}[n] = tr_1[n] + ts_1[n+1]$$

Now, expanding the intervals in the above equation using the definitions of the stimulus and response intervals of each oscillator, we get

$$P_{N-1}\left(1 + f_{N-1,1}(\varphi_{N-1}[n])\right) = P_1\left(1 - \varphi_1[n] + f_{1,N-1}(\varphi_1[n])\right) + P_1\varphi_1[n+1] \quad (4)$$

As mentioned earlier, we consider the synchrony to be the equilibrium state or steady state of the discrete map and thus using the definitions of phase at steady state, equation (4) becomes

$$P_{N-1}\left(1 + f_{N-1,1}(\varphi^*_{N-1})\right) = P_1\left(1 + f_{1,N-1}(\varphi^*_1)\right) \quad (5)$$

Now, using the phase approximation from the steady state and the linearized PRC about the steady state, equation (5) becomes

$$P_{N-1}\left(1 + f_{N-1,1}(\varphi_{N-1}^*) + f'_{N-1,1}(\varphi_{N-1}^*)\Delta\varphi_{N-1}[n]\right)$$
$$= P_1\left(1 - \varphi_1^* - \Delta\varphi_1[n] + f_{1,N-1}(\varphi_1^*) + f'_{1,N-1}(\varphi_1^*)\Delta\varphi_1[n]\right) + P_1\varphi_1^*$$
$$+ P_1\Delta\varphi_1[n+1]$$

Denoting $\mathrm{m}_1 = f'_{1,\mathrm{N}-1}(\varphi_1^*)$, $\mathrm{m}_{\mathrm{N}-1} = f'_{\mathrm{N}-1,1}(\varphi_{\mathrm{N}-1}^*)$, and cancelling the terms and using the steady state equation (5), we get

$$\Delta\varphi_{N-1}[n] = \frac{P_1}{P_{N-1}}\frac{1}{m_{N-1}}\left[(m_1 - 1)\Delta\varphi_1[n] + \Delta\varphi_1[n+1]\right] \quad (6)$$

Now, let us consider the main constraint (2). Rearranging the equation, we get

$$ts_1[n+1] = tr_{N-1}[n] + 2\delta - (ts_1[n] + tr_1[n])$$

Expressing the intervals in the above equation using phases and PRCs, we get

$$P_1(\varphi_1[n+1]) = P_{N-1}\left(1 - \varphi_{N-1}[n] + f_{N-1,1}(\varphi_{N-1}[n])\right) + 2\delta - P_1\left(1 + f_{1,N-1}(\varphi_1[n])\right)$$

At steady state, the above equation would be

$$P_1(\varphi_1^*) = P_{N-1}\left(1 - \varphi_{N-1}^* + f_{N-1,1}(\varphi_{N-1}^*)\right) + 2\delta - P_1\left(1 + f_{1,N-1}(\varphi_1^*)\right)$$

Now, approximating the phases about the steady state and linearizing the PRCs we get

$$P_1(\varphi_1^* + \Delta\varphi_1[n+1])$$
$$= 2\delta$$
$$+ P_{N-1}\left(1 - \varphi_{N-1}^* - \Delta\varphi_{N-1}[n] + f_{N-1,1}(\varphi_{N-1}^*) + f'_{N-1,1}(\varphi_{N-1}^*)\Delta\varphi_{N-1}[n]\right)$$
$$- P_1\left(1 + f_{1,N-1}(\varphi_1^*) + f'_{1,N-1}(\varphi_1^*)\Delta\varphi_1[n]\right)$$

Again, using the steady state equation and cancelling the terms, and denoting the slopes of the PRCs using m_1 and m_{N-1}, we get

$$P_1(\Delta\varphi_1[n+1]) = P_{N-1}(m_{N-1}-1)\Delta\varphi_{N-1}[n] - P_1 m_1 \Delta\varphi_1[n]$$

Rearranging, we get

$$\Delta\varphi_1[n+1] = \frac{P_{N-1}}{P_1}(m_{N-1}-1)\Delta\varphi_{N-1}[n] - m_1\Delta\varphi_1[n] \quad (9)$$

Now, substituting the expression for $\Delta\varphi_{\mathrm{N}-1}[\mathrm{n}]$ from equation (6) into equation (9), we get

$$\Delta\varphi_1[n+1] = \frac{P_{N-1}}{P_1}(m_{N-1}-1)\left\{\frac{P_1}{P_{N-1}}\frac{1}{m_{N-1}}\big((m_1-1)\Delta\varphi_1[n] + \Delta\varphi_1[n+1]\big)\right\} - m_1\Delta\varphi_1[n]$$

The periods get cancelled and multiplying the term m_{N-1} to the whole equation we get

$$m_{N-1}\Delta\varphi_1[n+1] = (m_{N-1}-1)[(m_1-1)\Delta\varphi_1[n] + \Delta\varphi_1[n+1]] - m_{N-1}m_1\Delta\varphi_1[n]$$

Rearranging the terms, we get

$$\Delta\varphi_1[n+1] = (m_{N-1}-1)(m_1-1)\Delta\varphi_1[n] - m_{N-1}m_1\Delta\varphi_1[n]$$

Simplifying the terms, we finally get the discrete linear map for the perturbation of the single oscillator that is perturbed:

$$\Delta\varphi_1[n+1] = (1 - m_1 - m_{N-1})\Delta\varphi_1[n] \quad (10)$$

The delay for a synchronous network can be calculated by substituting the delay δ for both the delays in equations (1) and (2) and solving for δ . Thus, we get,

$$\varphi_1^* = \frac{ts_1[\infty]}{P_1} = \frac{\delta}{P_1}$$

$$\varphi_{N-1}^* = \frac{ts_{N-1}[\infty]}{P_{N-1}} = \frac{\delta}{P_1\left(1 + f_{1,N-2}(\delta/P_1)\right)}$$

Substituting the values for the slopes of the PRCs, the map at a synchronous state is given by

$$\Delta\varphi_1[n+1] = 1 - f'_{1,N-1}\left(\frac{\delta}{P_i}\right) - f'_{N-1,1}\left(\frac{\delta}{P_1\left(\left(1 + f_{1,N-2}(\delta/P_1)\right)\right)}\right)$$

Since the PRC $f_{N-1,1}$is measured by simulating the unperturbed cluster using self-connections and delay, the slope $f'_{N-1,1}$ becomes a function of delay and thus the map becomes:

$$\Delta\varphi_1[n+1] = 1 - f'_{1,N-1}\left(\frac{\delta}{P_i}\right) - f'_{N-1,1,\delta}\left(\frac{\delta}{P_1\left(\left(1 + f_{1,N-2}(\delta/P_1)\right)\right)}\right)$$

Appendix B: Derivation for Stability of Clusters with Delays

From figure 5, we see that oscillators denoted by 1 and $A-1$ fire using the scheme where 1 fires first followed by $A-1$. After both have fired, their firing causes perturbation as input stimuli in the other cluster denoted by B in the order of their firing. However, between the two clusters A and B, the input perturbation due to one cluster follows immediately after firing, before the other cluster fires. Thus, when clusters 1 and $A-1$ fire one after the other, the phase of the oscillator B is linearly increasing until it receives both inputs after respective delays. Once B has received inputs from both sub-clusters, B fires, leading to input perturbations to sub-clusters 1 and $A-1$ after delay.

For convenience, we assume that the delays are small and are equal. We also assume that the periods P_1, P_{A-1} and P_B are equal. Even if we don't assume that the periods are same, at some point in the derivation of the map, they would cancel out. Hence, for convenience, we assume it early in the process.

Now, based on the figure 5, we write the necessary constraints to define the discrete map:

$$2\delta + tr_{A-1}[n] = ts_{B,1}[n] + ts_{B,A-1}[n] \qquad (1)$$

$$ts_{B,1}[n] = \delta + tr_{A-1}[n] + ts_{A-1,1}[n+1] \qquad (2)$$

$$ts_{A-1,B}[n+1] = ts_{B,A-1}[n] + tr_B[n] + \delta \qquad (3)$$

$$ts_{1,B}[n+1] = tr_B[n] + \delta \qquad (4)$$

$$ts_{B,1}[n] = 2\delta + tr_1[n] \qquad (5)$$

$$ts_{1,A-1}[n+1] = \delta + ts_{B,A-1}[n] \qquad (6)$$

Using the equation (1), and plugging in the expressions for stimulus and response intervals (and using the equality of intrinsic periods), we get

$$2\delta + \left(1 - \varphi_{A-1,B}[n] + f\left(\varphi_{A-1,B}[n]\right)\right) = \varphi_{B,1}[n] + \left(\varphi_{B,A-1}[n] - \varphi_{B,1}[n] + f\left(\varphi_{B,1}[n]\right)\right)$$

Here, as discussed in the results section, the steady state is the two-cluster solution, where each cluster has neurons that fire synchronously, but the two clusters need not necessarily synchronize with each other. With that as the steady-state, using the steady-state intervals and phases, and linearizing the PRCs about this fixed point, we get

$$\left(m_{A-1,B} - 1\right)\Delta\varphi_{A-1,B}[n] = \Delta\varphi_{B,A-1}[n] + m_{B,1}\Delta\varphi_{B,1}[n]$$

Rearranging the above equation, we get:

$$\Delta\varphi_{B,A-1}[n] = \left(m_{A-1,B} - 1\right)\Delta\varphi_{A-1,B}[n] - m_{B,1}\Delta\varphi_{B,1}[n] \qquad (7)$$

Now, using equation (5), we get a relation between $\Delta\varphi_{\mathrm{B},1}[\mathrm{n}]$ and $\Delta\varphi_{1,\mathrm{B}}[\mathrm{n}]$. Thus, substituting for the phases in (5), we get

$$\varphi_{B,1}[n] = 2\delta + \left(1 - \varphi_{1,B}[n] + f\left(\varphi_{1,B}\right)[n]\right)$$

Linearizing about the fixed points, we get

$$\Delta\varphi_{B,1}[n] = \left(m_{1,B} - 1\right)\Delta\varphi_{1,B}[n] \qquad (8)$$

Substituting equation (8) in equation (7), we get

$$\Delta\varphi_{B,A-1}[n] = \left(m_{A-1,B} - 1\right)\Delta\varphi_{A-1,B}[n] - m_{B,1}\left(m_{1,B} - 1\right)\Delta\varphi_{1,B}[n] \qquad (9)$$

Now, using equation (2), we get an expression for $\Delta\phi_{\mathrm{A-x,x}}[\mathrm{n}+1]$. Substituting phases in (2), we get

$$\varphi_{B,1}[n] = \delta + \left(1 - \varphi_{A-1,B}[n] + f\left(\varphi_{A-1,B}[n]\right)\right) + \varphi_{A-1,1}[n+1]$$

Linearizing about the fixed points, we get

$$\Delta\varphi_{B,1}[n] = \left(m_{A-1,B} - 1\right)\Delta\varphi_{A-1,B}[n] + \Delta\varphi_{A-1,1}[n+1]$$

Rearranging the above expression, we get

$$\Delta\varphi_{A-1,1}[n+1] = \Delta\varphi_{B,1}[n] - \left(m_{A-1,B} - 1\right)\Delta\varphi_{A-1,B}[n]$$

Substituting for $\varphi_{\mathrm{B},1}[\mathrm{n}]$ in the above equation from (8), we get

$$\Delta\varphi_{A-1,1}[n+1] = \left(m_{1,B} - 1\right)\Delta\varphi_{1,B}[n] - \left(m_{A-1,B} - 1\right)\Delta\varphi_{A-1,B}[n] \qquad (10)$$

Now, using equation (6), we get an expression for $\Delta\varphi_{1,\mathrm{A}-1}[\mathrm{n}+1]$. Substituting phases in (6), we get

$$\varphi_{1,A-1}[n+1] = \delta + \varphi_{B,A-1}[n] - \varphi_{B,1}[n] + f\left(\varphi_{B,1}[n]\right)$$

Linearizing the PRC about the fixed points, we get

$$\Delta\varphi_{1,A-1}[n+1] = \Delta\varphi_{B,A-1}[n] + \left(m_{B,1} - 1\right)\Delta\varphi_{B,1}[n]$$

Substituting for $\Delta\varphi_{\mathrm{B},\mathrm{A}-1}[\mathrm{n}]$ in the above equation from equation (9), we get

$$\Delta\varphi_{1,A-1}[n+1] = \left(m_{A-1,B} - 1\right)\Delta\varphi_{A-1,B}[n] - m_{B,1}\left(m_{1,B} - 1\right)\Delta\varphi_{1,B}[n] + \left(m_{B,1} - 1\right)\Delta\varphi_{B,1}[n]$$

Now, substituting for $\Delta\varphi_{\mathrm{B},1}[\mathrm{n}]$ in the above equation from equation (8), we get

$$\begin{aligned}\Delta\varphi_{1,A-1}[n+1] \\ &= \left(m_{A-1,B} - 1\right)\Delta\varphi_{A-1,B}[n] - m_{B,1}\left(m_{1,B} - 1\right)\Delta\varphi_{1,B}[n] \\ &+ \left(m_{B,1} - 1\right)\left(m_{1,B} - 1\right)\Delta\varphi_{1,B}[n]\end{aligned}$$

Rearranging and cancelling the terms, we get

$$\Delta\varphi_{1,A-1}[n+1] = \left(m_{A-1,B} - 1\right)\Delta\varphi_{A-1,B}[n] - \left(m_{1,B} - 1\right)\Delta\varphi_{1,B}[n] \qquad (11)$$

Now, let us consider equation (3) to get an expression for $\Delta\varphi_{\mathrm{A-1,B}}[\mathrm{n}+1]$. Substituting phases in (3), we get

$$\varphi_{A-1,B}[n+1] - \varphi_{A-1,1}[n+1] + f\left(\varphi_{A-1,1}[n+1]\right)$$
$$= \varphi_{B,A-1}[n] + \left(1 - \varphi_{B,A-1}[n] + f\left(\varphi_{B,A-1}[n]\right)\right) +$$

After cancelling and linearizing the PRCs about the fixed points, we get

$$\Delta\varphi_{A-1,B}[n+1] + \left(m_{A-1,1} - 1\right)\Delta\varphi_{A-1,1}[n+1] = \left(m_{B,1} - 1\right)\Delta\varphi_{B,1}[n] + m_{B,A-1}\Delta\phi_{B,A-1}[n]$$

Rearranging the above equation, we get

$$\Delta\varphi_{A-1,B}[n+1] = \left(m_{B,1} - 1\right)\Delta\varphi_{B,1}[n] - \left(m_{A-1,1} - 1\right)\Delta\varphi_{A-1,1}[n+1] + m_{B,A-1}\Delta\varphi_{B,A-1}[n]$$

Substituting for $\Delta\varphi_{\mathrm{A-1,1}}[\mathrm{n}+1]$ in the above equation from equation (10), we get

$$\Delta\varphi_{A-1,B}[n+1]$$
$$= m_{B,A-1}\Delta\varphi_{B,A-1}[n] + \left(m_{B,1} - 1\right)\Delta\varphi_{B,1}[n]$$
$$- \left(m_{A-1,1} - 1\right)\{\left(m_{1,B} - 1\right)\Delta\varphi_{1,B}[n] - \left(m_{A-1,B} - 1\right)\Delta\varphi_{A-1,B}[n]\}$$

Substituting for $\Delta\varphi_{\mathrm{B,1}}[\mathrm{n}]$ in the above equation from equation (8), we get

$$\Delta\varphi_{A-1,B}[n+1]$$
$$= m_{B,A-1}\Delta\varphi_{B,A-1}[n] + \left(m_{B,1} - 1\right)\left(m_{1,B} - 1\right)\Delta\varphi_{1,B}[n]$$
$$- \left(m_{A-1,1} - 1\right)\{\left(m_{1,B} - 1\right)\Delta\varphi_{1,B}[n] - \left(m_{A-1,B} - 1\right)\Delta\varphi_{A-1,B}[n]\}$$

Rearranging and simplifying, we get the following steps:

$$\Delta\varphi_{A-1,B}[n+1] = m_{B,A-1}\Delta\varphi_{B,A-1}[n] + (m_{1,B}-1)\big[(m_{B,1}-1)-(m_{A-1,1}-1)\big]\Delta\varphi_{1,B}[n] + (m_{A-1,1}-1)\{(m_{A-1,B}-1)\Delta\varphi_{A-1,B}[n]\}$$

$$\Delta\varphi_{A-1,B}[n+1] = m_{B,A-1}\Delta\varphi_{B,A-1}[n] + (m_{1,B}-1)\big[m_{B,1}-m_{A-1,1}\big]\Delta\varphi_{1,B}[n] + (m_{A-1,1}-1)(m_{A-1,B}-1)\Delta\varphi_{A-1,B}[n]$$

Now, we substitute for $\Delta\varphi_{\mathrm{B,A-1}}[\mathrm{n}]$ in the above equation from equation (9)

$$\Delta\varphi_{A-1,B}[n+1] = m_{B,A-1}\{(m_{A-1,B}-1)\Delta\varphi_{A-1,B}[n] - m_{B,1}(m_{1,B}-1)\Delta\varphi_{1,B}[n]\} + (m_{1,B}-1)\big[m_{B,1}-m_{A-1,1}\big]\Delta\varphi_{1,B}[n] + (m_{A-1,1}-1)(m_{A-1,B}-1)\Delta\varphi_{A-1,B}[n]$$

Rearranging the terms in the above equation, we get

$$\Delta\varphi_{A-1,B}[n+1] = \{m_{B,A-1}(m_{A-1,B}-1) + (m_{A-1,1}-1)(m_{A-1,B}-1)\}\Delta\varphi_{A-1,B}[n] + \{\big[m_{B,1}-m_{A-1,1}\big](m_{1,B}-1) - m_{B,A-1}m_{B,1}(m_{1,B}-1)\}\Delta\varphi_{1,B}[n]$$

Further rearranging the terms in the above equation gives us

$$\Delta\varphi_{A-1,B}[n+1] = (m_{A-1,B}-1)\{m_{B,A-1}+m_{A-1,1}-1\}\Delta\varphi_{A-1,B}[n] + (m_{1,B}-1)\{\big[m_{B,1}-m_{A-1,1}\big] - m_{B,A-1}m_{B,1}\}\Delta\varphi_{1,B}[n]$$

$$\Delta\varphi_{A-1,B}[n+1]$$
$$= \left(m_{A-1,B}-1\right)\{m_{B,A-1}+m_{A-1,1}-1\}\Delta\varphi_{A-1,B}[n]$$
$$+\left(m_{1,B}-1\right)\{m_{B,1}\left(1-m_{B,A-1}\right)-m_{A-1,1}\}\Delta\varphi_{1,B}[n]$$

Thus, we get the first equation of the map:

$$\Delta\varphi_{A-1,B}[n+1]$$
$$= \left(m_{A-1,B}-1\right)\{m_{B,A-1}+m_{A-1,1}-1\}\,\Delta\varphi_{A-1,B}[n]$$
$$+\left(m_{1,B}-1\right)\{m_{B,1}\left(1-m_{B,A-1}\right)-m_{A-1,1}\}\Delta\varphi_{1,B}[n] \quad (12)$$

Now, we use the constraint (4) to obtain the equation for $\varphi_{1,\mathrm{B}}[\mathrm{n}+1]$. Substituting the phases for the equation (4), we get

$$\varphi_{1,B}[n+1]-\varphi_{1,A-1}[n+1]+f\left(\varphi_{1,A-1}[n+1]\right)=1-\varphi_{B,A-1}[n]+f\left(\varphi_{B,A-1}[n]\right)+\ \delta$$

Linearizing the PRCs about the fixed points and cancelling the steady state terms, we get

$$\Delta\varphi_{1,B}[n+1]+\left(m_{1,A-1}-1\right)\Delta\varphi_{1,A-1}[n+1]=\left(m_{B,A-1}-1\right)\Delta\varphi_{B,A-1}[n]$$

Rearranging the above equation, we get

$$\Delta\varphi_{1,B}[n+1]=\left(m_{B,A-1}-1\right)\Delta\varphi_{B,A-1}[n]-\left(m_{1,A-1}-1\right)\Delta\varphi_{1,A-1}[n+1]$$

Substituting for $\varphi_{\mathrm{B,A-1}}[\mathrm{n}]$ from equation (9) and for $\varphi_{\mathrm{A-1,1}}[\mathrm{n}]$ from equation (11), we get

$$\Delta\varphi_{1,B}[n+1]=\left(m_{B,A-1}-1\right)\{\left(m_{A-1,B}-1\right)\Delta\varphi_{A-1,B}[n]-m_{B,1}\left(m_{1,B}-1\right)\Delta\varphi_{1,B}[n]\}$$
$$-\left(m_{1,A-1}-1\right)\{\left(m_{A-1,B}-1\right)\Delta\varphi_{A-1,B}[n]-\left(m_{1,B}-1\right)\Delta\varphi_{1,B}[n]\}$$

Rearranging the terms, we get

$$\Delta\varphi_{1,B}[n+1] = \{(m_{B,A-1}-1)(m_{A-1,B}-1) - (m_{1,A-1}-1)(m_{A-1,B}-1)\}\Delta\varphi_{A-1,B}[n]$$
$$+ \{(m_{1,A-1}-1)(m_{1,B}-1) - (m_{B,A-1}-1)m_{B,1}(m_{1,B}-1)\}\Delta\varphi_{1,B}[n]$$

Cancelling the terms and rearranging, we finally get the second equation of the map

$$\Delta\varphi_{1,B}[n+1] = (m_{A-1,B}-1)\{m_{B,A-1} - m_{1,A-1}\}\Delta\varphi_{A-1,B}[n] + (m_{1,B}-1)\{(m_{1,A-1}-1) - (m_{B,A-1}-1)m_{B,1}\}\Delta\varphi_{1,B}[n] \quad (13)$$

Like the results in the work of Chandrasekaran et.al, perhaps the intrinsic periods would have cancelled out even if we did not assume them to be equal. However, finally, the system (12) - (13) gives us a two-dimensional discrete linear system of the form:

$$\Delta[n+1] = S\Delta[n] \quad (14)$$

where S can be expressed as

$$\mathrm{S} = \begin{bmatrix} s_{11} & s_{12} \\ s_{21} & s_{22} \end{bmatrix} \quad (15)$$

The terms s_{11}, s_{12}, s_{21} and s_{22} are defined as

$$s_{11} = (m_{A-1,B}-1)\{m_{B,A-1} + m_{A-1,1} - 1\}$$

$$s_{12} = (m_{1,B}-1)\{m_{1,B,1}(1 - m_{1,B,A-1}) - m_{A-1,1}\}$$

$$s_{21} = (m_{A-1,B}-1)\{m_{B,A-1} - m_{1,A-1}\}$$

$$s_{22} = (m_{1,B}-1)\{(m_{1,A-1}-1) - (m_{B,A-1}-1)m_{B,1}\}$$

Based on this, the characteristic polynomial for the matrix (15) is given by

$$\lambda^2 - \lambda(s_{11} + s_{22}) + s_{11}s_{22} - s_{21}s_{12} = 0 \quad (16)$$

The stability of this cluster mode is determined by the eigen values of the characteristic polynomial given in equation (16). If $|\lambda_{\max}| < 1$, then we can conclude that the clustered solution is stable, implying that the applied perturbation decays to zero.

<u>Analysis of the Cluster Interaction Terms</u>

The perturbed sub-cluster 1 and the sub-cluster $A-1$ receive the same input from the other unperturbed cluster B. The sub-cluster $A-1$ is comprised of neurons identical to the neurons in the perturbed sub-cluster 1, but the response of each of the sub-clusters to an input from cluster B could differ because of other neurons on each other within each sub-cluster. We approximate the PRC for a cluster of identical neurons with that of an individual neuron. We presume that all post-synaptic oscillators comprised of identical neurons will have the same resetting irrespective of their composition in terms of the sub-cluster. Thus, the phase resetting for the sub-clusters 1 and $A-1$ for an input from B would be the same. Hence, we get the equality:

$$f_{A-1,B}\left(\varphi_{A-1,B}\right) = f_{1,B}\left(\varphi_{1,B}\right) = f_{A,B}(\varphi_A^*) \qquad (17)$$

This would result in the slopes being equal and we therefore get

$$m_{A-1,B} = m_{1,B} = m_{A,B}$$

Substituting these values in the 2-dimensional map (14), and solving the characteristic polynomial (15) for eigen values, we get the factorized characteristic polynomial as

$$(\lambda - \lambda_1)(\lambda - \lambda_2) = 0 \qquad (18)$$

where the λ_1 and λ_2 evaluated at phase-locked points are given by

$$\lambda_1 = \left(1 - f'_{A,B}(\varphi^*_A)\right)\left(1 - f'_{B,1}(\varphi^*_B)\right)\left(1 - f'_{B,A-1}(\varphi^*_B)\right) \tag{19}$$

$$\lambda_2 = \left(1 - f'_{A,B}(\varphi^*_A)\right)\left(1 - f'_{A-1,1}(\varphi^*_{A-1}) - f'_{1,A-1}(\varphi^*_1)\right) \tag{20}$$

λ_2 in equation (20) has the term $\left(1 - \mathrm{f}'_{\mathrm{A,B}}(\varphi^*_{\mathrm{A}})\right)$ that represents the effect of between cluster interactions on within cluster synchrony. Substituting the values of phases at steady state, we get

$$\lambda_1 = \left(1 - f'_{A,B}\left(\frac{ts^*{}_A}{P_A}\right)\right)\left(1 - f'_{B,1}\left(\frac{ts^*{}_{B,1}}{P_B}\right)\right)\left(1 - f'_{B,A-1}\left(\frac{ts^*{}_{B,A-1}}{P_B}\right)\right)$$

$$\lambda_2 = \left(1 - f'_{A,B}\left(\frac{ts^*{}_A}{P_A}\right)\right)\left(1 - f_{A-1,1}\left(\frac{ts^*{}_{A-1,1}}{P_{A-1}}\right) - f_{1,A-1}\left(\frac{ts^*{}_{1,A-1}}{P_1}\right)\right)$$